Physicochemical Properties and Structures of Room-Temperature Ionic Liquids. 3. Variation of Cationic Structures

Hiroyuki Tokuda,[†] Kunikazu Ishii,[†] Md. Abu Bin Hasan Susan,[†,||] Seiji Tsuzuki,[‡] Kikuko Hayamizu,[§] and Masayoshi Watanabe*[,†]

Department of Chemistry and Biotechnology, Yokohama National University and CREST-JST, 79-5 Tokiwadai, Hodogaya-ku, Yokohama 240-8501, Japan, and National Institute of Advanced Industrial Science and Technology, AIST Tsukuba Centre 2, Tsukuba 305-8568, Japan, and National Institute of Advanced Industrial Science and Technology, AIST Tsukuba Centre 5, Tsukuba 305-8565, Japan

Received: June 23, 2005; In Final Form: October 27, 2005

A series of room-temperature ionic liquids (RTILs) were prepared with different cationic structures, 1-butyl-3-methylimidazolium ([bmim]), 1-butylpyridinium ([bpy]), *N*-butyl-*N*-methylpyrrolidinium, ([bmpro]), and *N*-butyl-*N*,*N*,*N*-trimethylammonium ([(n-C_4H_9)$(CH_3)_3$N]) combined with an anion, bis(trifluoromethane sulfonyl)imide ([$(CF_3SO_2)_2$N]), and the thermal property, density, self-diffusion coefficients of the cation and anion, viscosity, and ionic conductivity were measured over a wide temperature range. The self-diffusion coefficient, viscosity, ionic conductivity, and molar conductivity follow the Vogel−Fulcher−Tamman equation for temperature dependencies, and the best-fit parameters have been estimated, together with the linear fitting parameters for the density. The relative cationic and anionic self-diffusion coefficients for the RTILs, independently determined by the pulsed-field-gradient spin−echo NMR method, appear to be influenced by the shape of the cationic structure. A definite order of the summation of the cationic and anionic diffusion coefficients for the RTILs: [bmim][$(CF_3SO_2)_2$N] > [bpy][$(CF_3SO_2)_2$N] > [bmpro][$(CF_3SO_2)_2$N] > [(n-C_4H_9)$(CH_3)_3$N][$(CF_3SO_2)_2$N], has been observed, which coincides with the reverse order to the viscosity data. The ratio of molar conductivity obtained from the impedance measurements to that calculated by the ionic diffusivity using the Nernst−Einstein equation quantifies the active ions contributing to ionic conduction in the diffusion components and follows the order: [bmpro][$(CF_3SO_2)_2$N] > [(n-C_4H_9)$(CH_3)_3$N][$(CF_3SO_2)_2$N] > [bpy][$(CF_3SO_2)_2$N] > [bmim][$(CF_3SO_2)_2$N] at 30 °C.

Introduction

A sufficient and systematic understanding of molecular structure-physicochemical properties relationship is a basic requirement for molecular design in chemistry with a view to creating new materials having desirable properties. Room-temperature ionic liquids (RTILs), so-called *designer solvents*, are composed entirely of ions, and their physicochemical properties can be easily tuned simply by changing the structure of the component ions.[1,2] Molecular design of the RTILs appears to be one of the most fascinating domains of current research, as reflected in the recent numerous studies.

Since the RTILs are room-temperature molten salts, the macroscopic physicochemical properties would be directly affected by their microscopic ion dynamics and ionic state. In addition to focusing on different combinations of new cations and anions to prepare novel RTILs and studies on their bulk physicochemical properties,[3−18] many research groups have explored microscopic information on the ions by spectroscopic methods, especially solvent−solute studies using a variety of solvatochromic probes.[19−24] Although investigation on the ion dynamics has also been available in the literature,[25−29] a systematic understanding on correlating them with the ionic structures and the bulk physicochemical properties is limited. Recently, we have applied the pulsed-field-gradient spin−echo (PGSE) NMR method for determination of the cationic and anionic self-diffusion coefficients of a wide variety of RTILs.[30,31] By study of the effect of the ionic structures on the physicochemical properties of a series of RTILs with a fixed cation, 1-butyl-3-methylimidazolium ([bmim]) with a wide variety of anions,[31a] as well as varying alkyl chain length attached to the imidazolium cation ([Rmim]) with bis(trifluoromethane sulfonyl)imide [$(CF_3SO_2)_2$N],[31b] we have been able to envisage a broad picture of the structural effects on the microscopic dynamics of the ions and their correlation with the macroscopic properties. A comprehensive understanding of the cationic structural effects on physicochemical properties would, therefore, underpin the knowledge on the structure−property relationship of RTILs.

From the first report of the RTIL, ethylammonium nitrate, in 1914 by Walden,[32] numerous cations combined with suitable anions have been discovered to be in the liquid state near or below ambient temperature, especially those including aromatic and aliphatic quaternary ammonium structures such as *N*, *N*′-dialkylimidazolium,[33,34] *N*-alkylpyridinium,[35] and tetraalkylammonium.[36−38] The large size of the organic cations is likely to reduce interionic electrostatic attraction, which would have the significant effect of lowering its melting point. The

* To whom correspondence should be addressed. E-mail: mwatanab@ynu.ac.jp. Fax: +81-45-339-3955.
† Yokohama National University.
‡ National Institute of Advanced Industrial Science and Technology, AIST Tsukuba Centre 2.
§ National Institute of Advanced Industrial Science and Technology, AIST Tsukuba Centre 5.
|| Present address: Department of Chemistry, University of Dhaka, Dhaka 1000, Bangladesh.

10.1021/jp053396f CCC: $33.50
Published on Web 01/26/2006

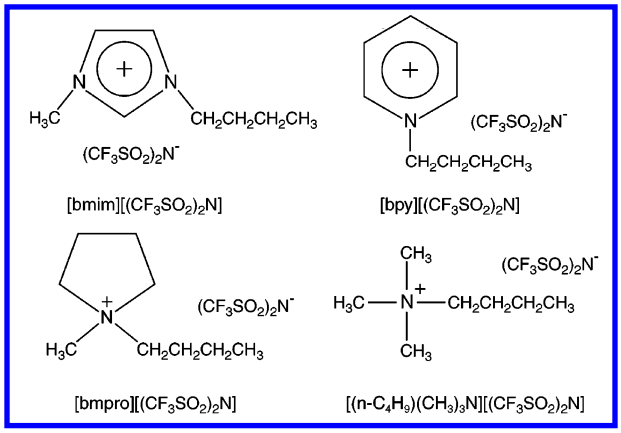

Figure 1. Molecular structures of $[bmim][(CF_3SO_2)_2N]$, $[bpy][(CF_3SO_2)_2N]$, $[bmpro][(CF_3SO_2)_2N]$, and $[(n\text{-}C_4H_9)(CH_3)_3N][(CF_3SO_2)_2N]$.

difference of electrostatic, inductive, and/or dispersive forces derived from variations of the cationic structures should also cause differences in physicochemical properties such as thermal properties, polarity, viscosity, and ionic diffusion behavior in each RTIL. However, the structural effects, such as aromatic or aliphatic, and linear or cyclic, for those properties are still unclear. In this study, we focus on a series of RTILs of quarternized ammonium cations with the same substituent butyl group: [bmim], *N*-butylpyridinium ([bpy]), *N*-butyl-*N*-methylpyrrolidinium ([bmpro]), and *N*-butyl-*N*,*N*,*N*,-trimethylammonium ($[(n\text{-}C_4H_9)(CH_3)_3N]$), with a fixed anion, $[(CF_3SO_2)_2N]$ (Figure 1). The physicochemical properties were explored with an emphasis on the ion-transport behavior, depending on the change in the cationic backbone structures, to understand the relationships between the ionic diffusivity, viscosity, and molar conductivity.

Experimental Section

Synthesis. In general, the synthesis of all the RTILs in this study involves a metathesis reaction of freshly prepared quaternized halide salts of the corresponding cationic structures with $LiN(SO_2CF_3)_2$, following a slightly modified procedure reported earlier.[3,5,16a] The preparation of $[bmim][(CF_3SO_2)_2N]$ and $[bpy][(CF_3SO_2)_2N]$ has been described in detail in our previous reports.[30,31] For other RTILs, the quarternized bromide salts were prepared, prior to the metathesis reaction. The bromide salt, [bmpro][Br], was prepared by reacting *N*-methylpyrrolidine with butylbromide in cyclohexane under a reflux condition, and the product was purified by recrystallization from 2-propanol/ethyl acetate to yield a white crystalline solid. The $[(n\text{-}C_4H_9)(CH_3)_3N][Br]$ was prepared by reacting trimethylamine and butylbromide in a water/acetone mixture, and after removal of the solvent, the crude product was recrystallized from 2-propanol/acetone. The ionic liquids, $[bmpro][(CF_3SO_2)_2N]$ and $[(n\text{-}C_4H_9)(CH_3)_3N][(CF_3SO_2)_2N]$, were prepared by anion exchange reaction of [bmpro][Br] and $[(n\text{-}C_4H_9)(CH_3)_3N][Br]$, respectively, with 1.2 equiv of $LiN(SO_2CF_3)_2$ in water, followed by repeatedly washing with water. After dehydration under high vacuum at 100 °C over 48 h, the ionic liquids, which were colorless liquids at room temperature, were finally stored in an argon atmosphere glovebox (VAC, $[O_2] < 1$ ppm, $[H_2O] < 1$ ppm).

The structures of the ionic liquids were identified by ^1H and ^{13}C NMR and fast atom bombardment mass spectra (FAB-MS). The RTILs were not miscible with water, and quantitative determination of the halide content was not feasible. However, halide in the aqueous phase in contact with the ionic liquids was not detectable by using an $AgNO_3$ aqueous solution, which indicates very low content of halide-based impurities, if any, in the prepared RTILs. FAB-MS spectra also showed no detectable impurities in each RTIL. Karl-Fisher titration was used for the determination of water content in the RTILs, and in all cases, the content was below 10 ppm.

TABLE 1: Molecular Weight and Thermal Properties

	Mw/g mol^{-1}	T_g/°C[a]	T_m/°C[a]	T_d/°C[b]
$[bmim][(CF_3SO_2)_2N]$	419.4	−87	−3	423
$[bpy][(CF_3SO_2)_2N]$	416.4	−76[c]	26	396
$[bmpro][(CF_3SO_2)_2N]$	422.4	−83	−15	431
$[(n\text{-}C_4H_9)(CH_3)_3N][(CF_3SO_2)_2N]$	396.4	−74	19	416

[a] Onset temperature of a heat capacity change (T_g) and an endothermic peak (T_m) determined by differential scanning calorimetry. [b] Onset temperatures of mass loss (T_d). [c] Detected by rapid cooling.

Measurements. Physicochemical properties of the RTILs were studied by the measurements of thermal behavior, density, self-diffusion coefficients of the cation and anion, viscosity, and ionic conductivity. The experimental details of the techniques used and measurements have been reported earlier[31a] and are briefly outlined here.

Differential scanning calorimetry (DSC) was carried out using a Seiko Instruments DSC 220C under nitrogen atmosphere. The samples were tightly sealed in Al pans, heated to 80 °C, followed by cooling to −150 °C, and then reheated to 100 °C at a cooling and heating rate of 10 °C min^{-1}. The glass transition temperature (T_g) and the melting point (T_m) were determined from the DSC thermograms during the programmed reheating steps.

Thermogravimetric measurements was carried out using a Seiko Instruments TG-DTA 6200 from room temperature to 550 °C at a heating rate of 10 °C min^{-1} under nitrogen atmosphere with open Al pans.

The density measurement was conducted using a thermoregulated density/specific gravity meter DA-100 (Kyoto Electronics Manufacturing Co. Ltd.) in the temperature range from 15 to 40 °C.

The PGSE-NMR measurement was conducted on a JEOL JNM-AL 400 spectrometer with a 9.4-T narrow-bore superconducting magnet equipped with a JEOL pulse field gradient probe and a current amplifier. The self-diffusion coefficients were determined by using a simple Hahn spin−echo sequence (i.e., 90°-τ-180°-τ-acquisition), incorporating a gradient pulse in each τ period. The interval of two gradient pulses, Δ, was set at 50 ms, and the duration of the field gradient, δ, was varied. The samples were inserted into a 5-mm (outside diameter) NMR microtube (BMS-005J, Shigemi, Tokyo), and the cationic and anionic self-diffusion coefficients in each RTIL were measured by using the ^1H (399.7 MHz) and ^{19}F (376.1 MHz) nuclei, respectively, in the temperature range of 80 to −10 °C with gradual cooling.

The viscosity of the RTILs was measured with a Toki RE80 cone-plate viscometer under nitrogen atmosphere in the temperature range of 10−80 °C.

The bulk ionic conductivity was determined by complex impedance measurements, using a computer-controlled Hewlett-Packard 4192A LF impedance analyzer over the frequency range from 5 Hz to 13 MHz. The measurements were carried out in a conductivity cell with platinized platinum electrodes (TOA Electronics, CG-511B) at controlled temperatures with cooling from 100 to −10 °C.

Results and Discussion

Thermal Property and Density. Table 1 lists the DSC results during the reheating scans. The RTILs in this study, except for

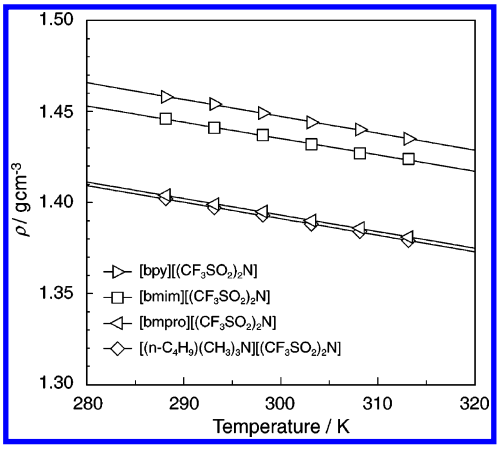

Figure 2. Density of $[(CF_3SO_2)_2N]$-based RTILs as a function of temperature.

TABLE 2: Density Equation Parameters and Molar Concentration at 30 °C (M_{30}) (Density Equation: $\rho = b - aT$)

	$a/10^{-4}$ g cm^{-3} K^{-1}	b/g cm^{-3}	$M_{30}/10^{-3}$ mol cm^{-3}
$[bmim][(CF_3SO_2)_2N]$	9.40	1.72	3.42
$[bpy][(CF_3SO_2)_2N]$	9.26	1.73	3.47
$[bmpro][(CF_3SO_2)_2N]$	9.09	1.67	3.29
$[(n\text{-}C_4H_9)(CH_3)_3N][(CF_3SO_2)_2N]$	9.09	1.66	3.50

$[bpy][(CF_3SO_2)_2N]$, exhibit a heat capacity change corresponding to the T_g in the DSC thermograms at the scanning rate of 10 °C min^{-1}, and the T_g ranges from −87 to −74 °C. At a scanning rate of 50 °C min^{-1}, a supercooling state could also be recognized for $[bpy][(CF_3SO_2)_2N]$, and the T_g could be determined as −76 °C. In the DSC trace at a scanning rate of 10 °C min^{-1} (data not shown), only an endothermic peak corresponding to T_m was detected for $[bmim][(CF_3SO_2)_2N]$ and $[bpy][(CF_3SO_2)_2N]$, while $[bmpro][(CF_3SO_2)_2N]$ exhibited two endothermic peaks at −25 and −15 °C and $[(n\text{-}C_4H_9)(CH_3)_3N][(CF_3SO_2)_2N]$ at 9 and 19 °C. It has been reported that these ionic liquids have multiendothermic peaks.[5c,d] On the other hand, Henderson et al. have pointed out to have only a single melting peak at −3 °C when the $[bmpro][(CF_3SO_2)_2N]$ fully crystallized by slow cooling.[39] This suggests that these ionic liquids have a possibility to have metastable crystalline phases, depending to the scanning rate. All of the ionic liquids, as apparent from the thermogravimetric results, show excellent short-term thermal stability up to ca. 400 °C. The onset temperature for the commencement of mass loss follows the order: [bmpro] > [bmim] > $[(n\text{-}C_4H_9)(CH_3)_3N]$ > [bpy]. The ionic liquid of the imidazolium cation has higher thermal stability compared to that of the alkylammonium cation, in good agreement with the literature;[11] however, interestingly, the thermal stability is surpassed by the ionic liquid based on the pyrrolidinium cation.

The density of the RTILs, as depicted in Figure 2, decreases linearly with increasing temperature. The best-fit parameters for the linear fitting of the temperatures dependencies of density are listed in Table 2. The aromatic cation-based RTILs show higher density than those based on the aliphatic cations, and the density follows the order: [bpy] > [bmim] > [bmpro] > $[(n\text{-}C_4H_9)(CH_3)_3N]$. The molar concentration of the RTILs at 30 °C (M_{30}) was calculated based on the density value and molecular weight and is also tabulated in Table 2. A decrease in the molecular weight mainly causes an increase in the molar concentration, which ranges from 3.29 to 3.50 mol L^{-1} for the RTILs in this study at 30 °C.

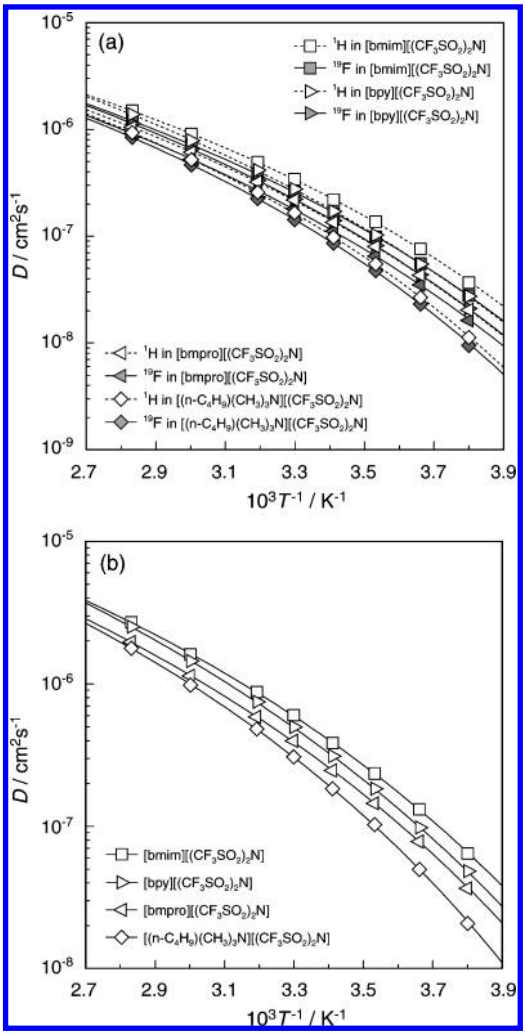

Figure 3. Temperature dependence of (a) self-diffusion coefficients of the cation and anion and (b) summation of the cationic and anionic self-diffusion coefficients ($D_{cation} + D_{anion}$) for $[(CF_3SO_2)_2N]$-based ionic liquids.

Ionic Diffusion Coefficient and Viscosity: Ion Transport Properties. The temperature dependency of self-diffusion coefficients of the cation (D_{cation}) and anion (D_{anion}) for $[bmim][(CF_3SO_2)_2N]$, $[bpy][(CF_3SO_2)_2N]$, $[bmpro][(CF_3SO_2)_2N]$, and $[(n\text{-}C_4H_9)(CH_3)_3N][(CF_3SO_2)_2N]$ is shown in Figure 3a. Figure 3b also exhibits the summation of the cationic and anionic self-diffusion coefficients ($D_{cation} + D_{anion}$) for these RTILs. Temperature dependencies of the self-diffusion coefficients have been fitted with the Vogel−Fulcher−Tamman (VFT) equation[40] for diffusivity

$$D = D_0 \exp[-B/(T - T_0)] \quad (1)$$

where the constants, D_0 (cm^2 s^{-1}), B (K), and T_0 (K) are adjustable parameters. Table 3 summarizes the best-fit parameters of the ionic diffusivity, and the dashed and solid lines in Figure 3 are the calculated curves by using the best-fit parameters and eq 1. The apparent cationic transference number ($D_{cation}/(D_{cation} + D_{anion})$) has been plotted as a function of temperature in Figure 4. Interestingly, the self-diffusion coefficient of the cation is found to be larger than that of the anion at all the temperatures of the measurements, an observation similar to our previous reports on [bmim]-based RTILs with different anionic structures and $[Rmim][(CF_3SO_2)_2N]$ ionic liquids with different alkyl chain length.[31] The difference in the

TABLE 3: VFT Equation Parameters of Self-Diffusion Coefficient Data ($D = D_0 \exp[-B/(T - T_0)]$)

	$D_0/10^{-4}$ cm^2 s^{-1}	$B/10^2$ K	T_0/K
	[bmim][$(CF_3SO_2)_2$N]		
cation	1.1 ± 0.1	8.45 ± 0.37	157 ± 3
anion	1.3 ± 0.3	9.33 ± 0.67	152 ± 6
cation + anion	2.3 ± 0.3	8.84 ± 0.45	155 ± 4
	[bpy][$(CF_3SO_2)_2$N]		
cation	2.0 ± 0.4	10.17 ± 0.69	149 ± 6
anion	1.6 ± 0.0	10.01 ± 0.06	151 ± 0
cation + anion	3.6 ± 0.4	10.10 ± 0.37	150 ± 3
	[bmpro][$(CF_3SO_2)_2$N]		
cation	1.1 ± 0.2	9.07 ± 0.54	157 ± 5
anion	1.3 ± 0.2	10.02 ± 0.39	151 ± 3
cation + anion	2.3 ± 0.3	9.51 ± 0.42	154 ± 4
	[(n-C_4H_9)$(CH_3)_3$N][$(CF_3SO_2)_2$N]		
cation	1.2 ± 0.2	9.14 ± 0.46	164 ± 4
anion	1.3 ± 0.1	9.61 ± 0.35	161 ± 3
cation + anion	2.4 ± 0.3	9.36 ± 0.39	163 ± 3

size of the cation and anion contributes to different self-diffusion coefficients of the cation and anion for the RTILs, as reported earlier.[31] However, the van der Waals volumes of [bmpro], [bmim], [bpy], [(n-C_4H_9)$(CH_3)_3$N], and [$(CF_3SO_2)_2$N] are 167, 150, 148, 144, and 147 Å^3 (0.342, 0.330, 0.328, 0.325, and 0.327 nm in radius), respectively,[41,42] and the ionic size effects on the transference number does not hold for the present series of ionic liquids with approximately the same cationic size. The order of the cationic transference number: [bmim] > [bpy] > [bmpro] > [(n-C_4H_9)$(CH_3)_3$N] is, therefore, influenced not only by size of the ions but also by other parameters, such as shape of the cations and local interaction between the cations and the anion.

Figure 5 depicts temperature dependency of the viscosity (η) for the RTILs along with the calculated lines, based on the VFT equation for viscosity and the best-fit parameters (Table 4). The corresponding VFT equation is

$$\eta = \eta_0 \exp[B/(T - T_0)] \quad (2)$$

where η_0 (mPa s), B (K), and T_0 (K) are constants. The relatively high viscosity of the ionic liquids from 40.0 to 76.6 mPa s at 30 °C is well justified in terms of their low diffusion coefficients of the sum of the cation and anion (from 3.1 to 6.0 × 10^{-7} cm^2 s^{-1} at 30 °C). In the temperature range of measurements, the macroscopic viscosity values follow the order: [(n-C_4H_9)-

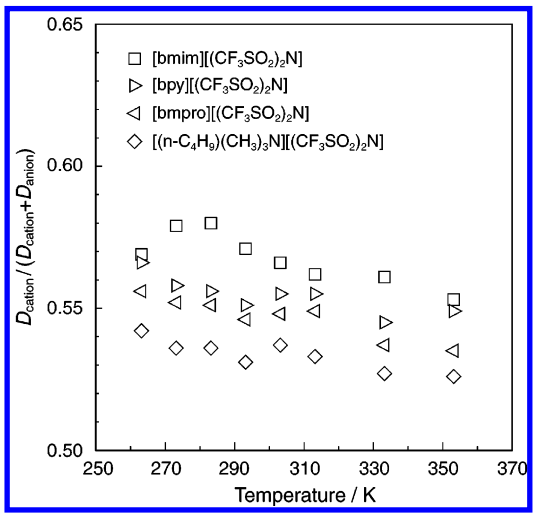

Figure 4. Apparent cationic transference number, $D_{cation}/(D_{cation} + D_{anion})$, for [$(CF_3SO_2)_2$N]-based RTILs plotted against temperature.

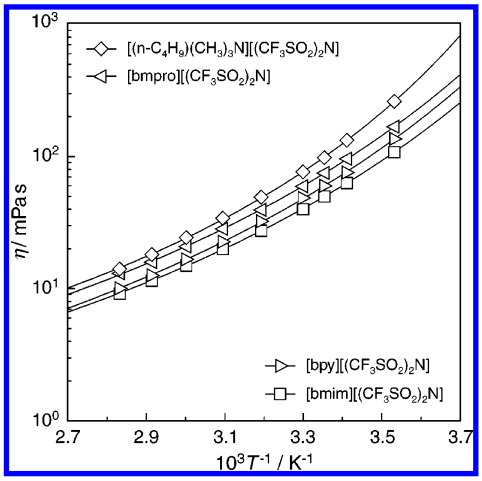

Figure 5. Viscosity of [$(CF_3SO_2)_2$N]-based RTILs as a function of temperature.

TABLE 4: VFT Equation Parameters of Viscosity Data ($\eta = \eta_0 \exp[B/(T - T_0)]$)

	$\eta_0/10^{-1}$ mPa s	$B/10^2$ K	T_0/K
[bmim][$(CF_3SO_2)_2$N]	2.5 ± 0.2	6.25 ± 0.22	180 ± 2
[bpy][$(CF_3SO_2)_2$N]	2.1 ± 0.4	6.71 ± 0.52	179 ± 5
[bmpro][$(CF_3SO_2)_2$N]	2.9 ± 0.4	6.51 ± 0.31	181 ± 3
[(n-C_4H_9)$(CH_3)_3$N][$(CF_3SO_2)_2$N]	4.5 ± 0.6	5.34 ± 0.27	199 ± 3

$(CH_3)_3$N][$(CF_3SO_2)_2$N] > [bmpro][$(CF_3SO_2)_2$N] > [bpy][$(CF_3SO_2)_2$N] > [bmim][$(CF_3SO_2)_2$N], which coincides with the reverse order of the ionic self-diffusion coefficients. The contrastive features of the viscosity with ionic diffusivity agree well with our observations for [bmim]-based RTILs with different anionic structures and [Rmim][$(CF_3SO_2)_2$N] ionic liquids with different alkyl chain length,[31] and thus, the microscopic ion dynamics reflects the macroscopic physical properties.

Ionic Conductivity and Diffusion Coefficient: Cationic Structural Effects on Ionic Association. The RTILs have relatively high ionic conductivity (σ), which exhibits temperature dependency as depicted in Figure 6. The VFT equation for conductivity is

$$\sigma = \sigma_0 \exp[-B/(T - T_0)] \quad (3)$$

where σ_0 (S cm^{-1}), B (K), and T_0 (K) are constants. The best-

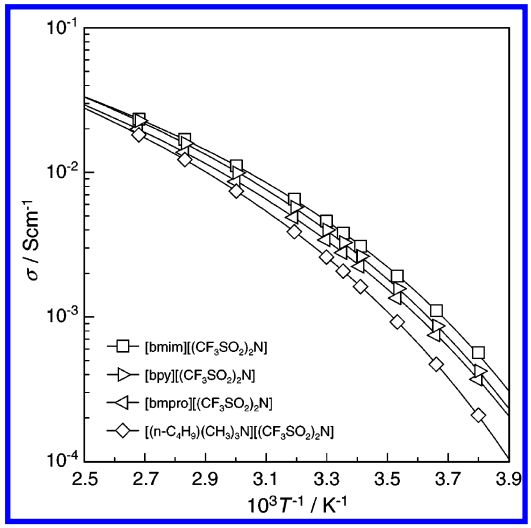

Figure 6. Temperature dependence of ionic conductivity for [$(CF_3SO_2)_2$N]-based RTILs.

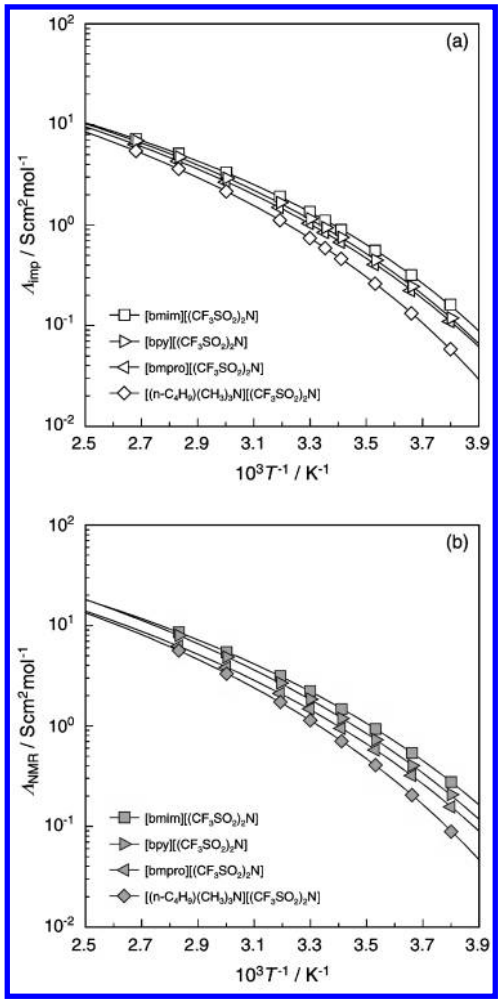

Figure 7. Molar conductivity of $[(CF_3SO_2)_2N]$-based RTILs: (a) obtained from ionic conductivity and molar concentration; (b) calculated from ionic self-diffusion coefficients and the Nernst−Einstein equation.

TABLE 5: VFT Equation Parameters of Ionic Conductivity Data ($\sigma = \sigma_0 \exp[-B/(T - T_0)]$)

	$\sigma_0/10^{-1}$ S cm^{-1}	$B/10^2$ K	T_0/K
[bmim][$(CF_3SO_2)_2$N]	4.3 ± 0.2	5.65 ± 0.14	178 ± 2
[bpy][$(CF_3SO_2)_2$N]	5.5 ± 0.5	6.33 ± 0.24	175 ± 3
[bmpro][$(CF_3SO_2)_2$N]	5.6 ± 0.2	6.75 ± 0.14	171 ± 1
[(n-C_4H_9)$(CH_3)_3$N][$(CF_3SO_2)_2$N]	6.1 ± 0.1	6.89 ± 0.04	177 ± 0

fit parameters are tabulated in Table 5. The σ for the ionic liquids follows the order: [bmim][$(CF_3SO_2)_2$N] > [bpy][$(CF_3SO_2)_2$N] > [bmpro][$(CF_3SO_2)_2$N] > [(n-C_4H_9)$(CH_3)_3$N][$(CF_3SO_2)_2$N. Although the molar concentration of these RTILs is dependent on the cationic structures (Table 2), the molar conductivity calculated from the ionic conductivity and the molar concentration (Figure 7a) follows the same order as for the ionic conductivity, which agrees well with the order of the ionic self-diffusion coefficient. The VFT equation for the molar conductivity is

$$\Lambda = \Lambda_0 \exp[-B/(T - T_0)] \quad (4)$$

where Λ_0 (S cm^2 mol^{-1}), B (K), and T_0 (K) are constants. Table 6 lists the best-fit parameters for the VFT equation. The molar conductivity based on the PGSE-NMR diffusivity (Λ_{NMR}) could also be calculated by using the Nernst−Einstein equation

$$\Lambda_{NMR} = N_A e^2 (D_{cation} + D_{anion})/kT = F^2 (D_{cation} + D_{anion})/RT \quad (5)$$

TABLE 6: VFT Equation Parameters of Molar Conductivity Data

	$\Lambda_0/10^2$ S cm^2 mol^{-1}	$B/10^2$ K	T_0/K
$\Lambda_{imp} = \Lambda_0 \exp[-B/(T - T_0)]$			
[bmim][$(CF_3SO_2)_2$N]	1.5 ± 0.1	6.05 ± 0.13	175 ± 1
[bpy][$(CF_3SO_2)_2$N]	2.0 ± 0.2	6.75 ± 0.27	172 ± 3
[bmpro][$(CF_3SO_2)_2$N]	2.1 ± 0.1	7.21 ± 0.16	168 ± 2
[(n-C_4H_9)$(CH_3)_3$N][$(CF_3SO_2)_2$N]	2.2 ± 0.3	7.31 ± 0.04	174 ± 0
$\Lambda_{NMR} = \Lambda_0 \exp[-B/(T - T_0)]$			
[bmim][$(CF_3SO_2)_2$N]	3.6 ± 0.4	7.03 ± 0.33	165 ± 3
[bpy][$(CF_3SO_2)_2$N]	5.4 ± 0.5	8.18 ± 0.28	160 ± 3
[bmpro][$(CF_3SO_2)_2$N]	3.6 ± 0.4	7.65 ± 0.30	164 ± 3
[(n-C_4H_9)$(CH_3)_3$N][$(CF_3SO_2)_2$N]	3.8 ± 0.4	7.67 ± 0.27	171 ± 2

where N_A is the Avogadro number, e is the electric charge on each ionic carrier, k is the Boltzmann constant, F is the Faraday constant, and R is the universal gas constant. Figure 7b shows the temperature dependency of the molar conductivity calculated from the ionic diffusion coefficient and eq 5, and Table 6 lists the best-fit parameters of the VFT equation. The calculated molar conductivity (Λ_{NMR}) is always higher than that of the experimental molar conductivity (Λ_{imp}) in the whole temperature range. The PGSE-NMR self-diffusion coefficients denote translational motion (self-diffusion) of the NMR sensitive nuclei. Thus, the Λ_{NMR} values are derived from the assumption that all of the diffusing species detected by the PGSE-NMR measurement contribute to the molar conductivity. On the other hand, the Λ_{imp} values (direct current (d.c.) conductivity) are based on the migration of the charged species under an electric field. The $\Lambda_{imp}/\Lambda_{NMR}$, therefore, indicates the percentage of ions (charged species) contributing to the ionic conduction in the diffusing species. It should be noted here that we could not distinguish the difference in the NMR chemical shifts between free ions and associated ionic species within the NMR time scale (10^{-9}−10^{-10} s). This implies that the association/dissociation rate of the ionic species, if any, is much faster than the time scale of the d.c. conductivity measurements. In the time scale of the conductivity measurements, an individual ion migrates under an electric field for a certain period when it exists as a charged species, but it may associate to form noncharged pairs and aggregates for another certain period. When the ion exists as a noncharged species, it does not contribute to the d.c conduction. Thus, the $\Lambda_{imp}/\Lambda_{NMR}$ ratios can be a measure for ionic association of the RTIL.

Figure 8 displays the $\Lambda_{imp}/\Lambda_{NMR}$ plotted against temperature, which is found to be relatively insensitive to the temperature. The ratios for all of the RTILs in this study are lower than unity, indicating that not all of the diffusive species in the ionic liquids contribute to the ionic conduction and that ionic association seems to occur in the system. Formation of such ion aggregates and/or clusters could also be observed in the FAB-MS results for all of the ionic liquids. For instance in the FAB-MS for [bpy][$(CF_3SO_2)_2$N], the mass-to-charge ratio, $m/z = 136$ (relative intensity, $I = 100\%$) and 552 (0.5%) in the positive mode can be assigned to the quasimolecular ion peaks of [bpy] and [bpy]$_2$-[$(CF_3SO_2)_2$N], respectively. The $m/z = 280$ ($I = 100\%$), 696 (0.6%), and 1112 (0.01%) in the negative FAB spectrum correspond to the [$(CF_3SO_2)_2$N], [bpy][$(CF_3SO_2)_2$N]$_2$, and [bpy]$_2$[$(CF_3SO_2)_2$N]$_3$, respectively. Since the anionic species and the substituent alkyl chain length of the RTILs in this study are fixed, the order of the $\Lambda_{imp}/\Lambda_{NMR}$ may simply depend on the nature of the cationic structures. The molar conductivity ratio follows the order: [bmpro] > [(n-C_4H_9)$(CH_3)_3$N] > [bpy] > [bmim], and interestingly, higher $\Lambda_{imp}/\Lambda_{NMR}$ values are observed for the aliphatic cations rather than their aromatic counterparts.

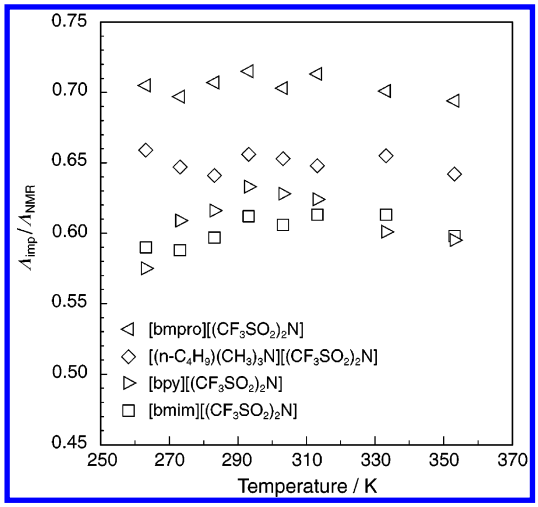

Figure 8. Molar conductivity ratios ($\Lambda_{imp}/\Lambda_{NMR}$) for $[(CF_3SO_2)_2N]$-based RTILs plotted against temperature.

The variation in the cationic structures leads to varying interactive forces, originated from the difference in the geometrical shape, steric hindrance, and the acidity of the individual interacting sites, causing a difference in polarity for each RTIL. The empirical polarity scale for electron-pair acceptor ability, $E_T(30)$, or normalized scale, E_T^N, has been most widely used for the direct correlation of microscopic solvent−solute interactions in several RTILs by solvatochromic polarity measurements.[19−24,43,44] This is based on the large blue solvatochromic shift of the long-wavelength intramolecular $\pi-\pi^*$ charge-transfer absorption band of Reichardt's betaine dye.[45] The solvatochromic shift can diagnose the effects arising from solvent polarizability, hydrogen bonding, and Lewis acidity, with the greatest contribution from the hydrogen-bond donor (HBD) property (proton donor ability of solvents). The [bmim][$(CF_3SO_2)_2N$] ionic liquid gave higher value of the E_T^N and the Kamlet−Taft parameter,[46] α, representing the higher HBD ability, compared to those for [bmpro][$(CF_3SO_2)_2N$].[23] The higher $E_T(30)$ value of [bmim][BF_4] compared to [bpy][BF_4] was also reported in the literature,[20,23] and this tendency may hold for the RTILs in our study despite the difference in the anionic species. The order of the polarity ($E_T(30)$ or E_T^N) has been found to contrast with that of the $\Lambda_{imp}/\Lambda_{NMR}$ for the present RTILs, which will be reported elsewhere.

We have also reported the intermolecular interaction energies of nine ion pairs of RTILs by the high level ab initio calculation.[47] The interaction energies (E_{int}) of [BF_4] with 1-ethyl-3-methylimidazolium ([emim]), 1-ethylpyridinium ([epy]), *N*-ethyl-*N*-methylpyrrolidinium ([empro]), and *N*-ethyl-*N*,*N*,*N*-trimethylammonium ([$(C_2H_5)(CH_3)_3N$]) are similar (−85.2, −82.8, −84.4, and −84.6 kcal mol^{-1}, respectively). However, the magnitude of orientation dependence of the interaction energy (E_{diff}), determined by the difference in the E_{int} values between the most stable and the least stable geometry, follows the order: [emim] > [epy] ≈ [$(C_2H_5)(CH_3)_3N$] > [empro]. Although the calculated RTILs and the present ones have differences in terms of the anionic structure and alkyl chain length of the cations, the order of the E_{diff} agrees with the reverse order of $\Lambda_{imp}/\Lambda_{NMR}$ for the present ionic liquids. Since the aromatic plane structures can realize close contacts with the anion, the positive charge distribution on the [emim] and [epy] would be a cause of the most stable geometries of these ion-pairs. For the [emim] ion pair, the anion prefers to have a close contact with the C_2-H on the imidazolium ring, which would be attributed to the larger positive charge on the C_2-H than the C_4-H and C_5-H. Similarly, for the [epy] ion pair, the anion is likely to locate around the nitrogen atom, C_2-H, and C_6-H. On the other hand, the aliphatic [empro] and [$(C_2H_5)(CH_3)_3N$] maintain relatively larger cation−anion distances than the aromatic ones, possibly because the cationic geometries prohibit to have close contacts with the anion due to their steric hindrance. The [empro] ion pair shows large numbers of isoenergetic local minima, relative to the other cations, which would contribute to the largest $\Lambda_{imp}/\Lambda_{NMR}$ value among the present RTILs.

Concluding Remarks

By analysis of the physicochemical properties of the RTILs with varying ionic structures, we have been able to reveal a broad picture of the ionic transport behavior and to recognize the interrelating parameters dominating the behavior in the system. The microscopic ionic diffusion is significantly influenced not only by the relative cationic and anionic size but also by the geometric shape. The contrastive feature between ionic diffusion coefficients, obtained from the PGSE-NMR measurements, and macroscopic viscosity indicates that the microscopic ion dynamics and ionic state significantly contributes to the macroscopic physicochemical properties of the ionic liquids. The apparent degree of the dissociation, quantified as the molar conductivity ratio ($\Lambda_{imp}/\Lambda_{NMR}$), changes depending on the cationic structures and is interestingly larger for the aliphatic cations ([bmpro] and [$(n-C_4H_9)(CH_3)_3N$]), compared with the aromatic counterparts ([bmim] and [bpy]).

Acknowledgment. This research was supported in part by Grant-in-Aid for Scientific Research (A-16205024 and 452-17073009) from the MEXT. The authors acknowledge Mr. Takeo Kaneko (YNU) for FAB-MS measurements. H.T. and M.A.B.H.S. acknowledge JSPS, and K.H. acknowledges NEDO for financial support.

References and Notes

(1) (a) Seddon, K. R. *J. Chem. Technol. Biotechnol.* **1997**, *68*, 351−356. (b) Freemantle, M. *Chem. Eng. News* **1998**, *76*, 32−37. (c) Freemantle, M. *Chem., & Eng. News* **2000**, *78*, 37−50. (d) Freemantle, M. *Chem. Eng. News* **2001**, *79*, 21−25.

(2) (a)Welton, T. *Chem. Rev.* **1999**, *99*, 2071−2083. (b)Holbrey, J. D.; Seddon, K. R. *Clean Prod. Process.* **1999**, *1*, 223−236. (c) Wassersheid, P.; Keim, W. *Angew. Chem., Int. Ed.* **2000**, *39*, 3772−3789. (d) Wilkes, J. S. *J. Mol. Catal. A Chem.* **2004**, *214*, 11−17.

(3) Bonhôte, P.; Dias, A.-P.; Papageorgiou, N.; Kalyanasundaram, K.; Grätzel, M. *Inorg. Chem.* **1996**, *35*, 1168−1178.

(4) (a) Holbrey, J. D.; Seddon, K. R. *Clean Prod. Process.* **1999**, *1*, 223−236. (b) Holbrey, J. D.; Seddon, K. R. *J. Chem. Soc., Dalton Trans.* **1999**, 2133−2139.

(5) (a) Sun, J.; MacFarlane, D. R.; Forsyth, M. *Ionics* **1997**, *3*, 356−362. (b) Sun, J.; Forsyth, M.; MacFarlane, D. R. *J. Phys. Chem. B* **1998**, *102*, 8858−8864. (c) MacFarlane, D. R.; Meakin, P.; Sun, J.; Amini, N.; Forsyth, M. *J. Phys. Chem. B* **1999**, *103*, 4164−4170. (d) MacFarlane, D. R.; Meakin, P.; Amini, N.; Forsyth, M. *J. Phys.: Condens. Matter* **2001**, *13*, 8257−8267.

(6) (a) MacFarlane, D. R.; Forsyth, S. A.; Golding, J.; Deacon, G. B. *Green Chem.* **2002**, *4*, 444−448. (b) Pringle, J. M.; Golding, J.; Forsyth, C. M.; Deacon, G. B.; Forsyth, M.; MacFarlane, D. R. *J. Mater. Chem.* **2002**, *12*, 3457−3480.

(7) Forsyth, S. A.; MacFarlane, D. R. *J. Mater. Chem.* **2003**, *13*, 2451−2456.

(8) (a) Matsumoto, H.; Yanagida, M.; Tanimoto, K.; Nomura, M.; Kitagawa, Y.; Miyazaki, Y. *Chem. Lett.* **2000**, 922−923. (b) Matsumoto, H.; Matsuda, T.; Miyazaki, Y. *Chem. Lett.* **2000**, 1430−1431. (c) Matsumoto, H.; Kageyama, H.; Miyazaki, Y. *Chem. Lett.* **2001**, 182−183.

(9) (a) Zhou, Z.-B.; Takeda, M.; Ue, M. *J. Fluorine Chem.* **2004**, *125*, 471−476. (b) Zhou, Z.-B.; Matsumoto, M.; Tatsumi, K. *Chem. Lett.* **2004**, 680−681. (c) Zhou, Z.-B.; Matsumoto, M.; Tatsumi, K. *Chem. Lett.* **2004**, 886−887.

(10) (a) Koch, V. R.; Dominey, L. A.; Nanjundiah, C.; Ondrechen, J. *J. Electrochem. Soc.* **1996**, *143*, 798−803. (b) Nanjundiah, C.; McDevitt, S. F.; Koch, V. R. *J. Electrochem. Soc.* **1997**, *144*, 3392−3397. (c) MacEwen, A. B.; Ngo, H. L.; LeCompte, K.; Goldman, J. L. *J. Electrocehm. Soc.* **1999**, *146*, 1687−1695.

(11) Ngo, H. L.; LeCompte, K.; Hargen, L.; McEwen, A. B. *Thermochim. Acta* **2000**, *357*−*358*, 97−102.

(12) (a) Fox, D. M.; Awad, W. H.; Gilman, J. W.; Maupin, P. H.; DeLong, H. C.; Trulove, P. C. *Green Chem.* **2003**, *5*, 724−727. (b) Awad, W. H.; Gilman, J. W.; Nyden, M.; Harris, R. H.; Sutto, T. E.; Callahan, J.; Trulove, P. C.; DeLong, H. C.; Fox, D. M. *Thermochim. Acta* **2004**, *409*, 3−11.

(13) Huddleston, J. G.; Visser, A. E.; Reichart, W. M.; Willauer, H. D.; Broker, G. A.; Rogers, R. D. *Green Chem.* **2001**, *3*, 156−164.

(14) Hagiwara, R.; Matsumoto, K.; Nakamori, Y.; Tsuda, T.; Ito, Y.; Matsumoto, H.; Momota, K. *J. Electrochem. Soc.* **2003**, *150*, D195−D199.

(15) (a) Xu, W.; Cooper, E. I.; Angell, C. A. *J. Phys. Chem. B* **2003**, *107*, 6170−6178. (b) Xu, W.; Wang, L.-M.; Nieman, R. A.; Angell, C. A. *J. Phys. Chem. B* **2003**, *107*, 11749−11756.

(16) (a) Cammarata, L.; Kazarian, S. G.; Salter, P. A.; Welton, T. *Phys. Chem. Chem. Phys.* **2001**, *3*, 5192−5200. (b) Seddon, K. R.; Stark, A.; Torres, M. J. *Pure Appl. Chem.* **2000**, *72*, 2275−2287.

(17) (a) Armstrong, D. W.; He, L.; Liu, Y.-S. *Anal. Chem.* **1999**, *71*, 3873−3876. (b) Anthony, J. L.; Maginn, E. J.; Brennecke, J. F. *J. Phys. Chem. B* **2001**, *105*, 10942−10949. (c) Blanchard, L. A.; Gu, Z.; Brennecke, J. F. *J. Phys. Chem. B* **2001**, *105*, 2437−2444.

(18) Lancaster, N. L.; Salter, P. A.; Welton, T.; Young, G. B. *J. Org. Chem.* **2002**, *67*, 8855−8861.

(19) Carmichael, A. J.; Seddon, K. R. *J. Phys. Org. Chem.* **2000**, *13*, 591−595.

(20) Aki, S. N. V. K.; Brennecke, J. F.; Samanta, A. *Chem. Commun.* **2001**, 413−414.

(21) Muldoon, M. J.; Gordon, C. M.; Dunkin, I. R. *J. Chem. Soc., Perkin Trans. 2* **2001**, 433−435.

(22) Dzyuba, S. V.; Bartsch, R. A. *Tetrahedron Lett.* **2002**, *43*, 4657−4659.

(23) Crowhurst, L.; Mawdsley, P. R.; Arlandis, J. M. P.; Salter, P. A.; Welton, T. *Phys. Chem. Chem. Phys.* **2003**, *5*, 2790−2794.

(24) Fletcher, K. A.; Pandey, S. *J. Phys. Chem. B* **2003**, *107*, 13532−13539.

(25) Baker, S. N.; Baker, G. A.; Kane, M. A.; Bright, F. V. *J. Phys. Chem. B* **2001**, *105*, 9663−9668.

(26) (a) Karmakar, R.; Samanta, A. *J. Phys. Chem. A* **2002**, *106*, 4447−4452. (b) Karmakar, R.; Samanta, A. *J. Phys. Chem. A* **2002**, *106*, 6670−6675.

(27) Ingram, J. A.; Moog, R. S.; Ito, N.; Biswas, R.; Maroncelli, M. *J. Phys. Chem. B* **2003**, *107*, 5926−5932.

(28) Baker, S. N.; Baker, G. A.; Munson, C. A.; Chen, F.; Bukowski, E. J.; Cartwright, A. N.; Bright, F. V. *Ind. Eng. Chem. Res.* **2003**, *42*, 6457−6463.

(29) Hyun, B.-R.; Dzyuba, S. V.; Bartsch, R. A.; Quitevis, E. L. *J. Phys. Chem. A* **2002**, *106*, 7579−7585.

(30) Noda, A.; Hayamizu, K.; Watanabe, M. *J. Phys. Chem. B* **2001**, *105*, 4603−4610.

(31) (a) Tokuda, H.; Hayamizu, K.; Ishii, K.; Susan, M. A. B. H.; Watanabe, M. *J. Phys. Chem. B* **2004**, *108*, 16593−16600. (b) Tokuda, H.; Hayamizu, K.; Ishii, K.; Susan, M. A. B. H.; Watanabe, M. *J. Phys. Chem. B* **2005**, *109*, 6103−6110.

(32) Walden, P. *Bull. Acad. Sci.* **1914**, 405−422.

(33) (a) Wilkes, J. S.; Levisky, J. A.; Wilson, R. A.; Hussey, C. L. *Inorg. Chem.* **1982**, *21*, 1263−1264. (b) Fannin, A. A.; King, L. A.; Levinsky, J. A.; Wilkes, J. S. *J. Phys. Chem.* **1984**, *88*, 2609−2614. (c) Fannin, A. A.; Floreani, D. A.; King, L. A.; Landers, J. S.; Piersma, B. J.; Stech, D. J.; Vaughn, R. L.; Wilkes, J. S.; Williams, J. L. *J. Phys. Chem.* **1984**, *88*, 2614−2621.

(34) Wilkes, J. S.; Zaworotko, M. J. *J. Chem. Soc. Chem. Commun.* **1992**, 965−967.

(35) (a) Chum, H. L.; Koch, V. R.; Miller, L. L.; Osteryoung, R. A. *J. Am. Chem. Soc.* **1975**, *97*, 3264−3265. (b) Gale, R. J.; Gilbert, B.; Osteryoung, R. A. *Inorg. Chem.* **1978**, *17*, 2728−2729. (c) Robinson, J.; Osteryoung, R. A. *J. Am. Chem. Soc.* **1979**, *101*, 323−327.

(36) Swan, G. C.; Ohno, A.; Roe, D. K.; Brown, R.; Maugh, T. *J. Am. Chem. Soc.* **1967**, *89*, 2648−2649.

(37) (a) Ford, W. T.; Hauri, R. J.; Hart, D. J. *J. Org. Chem.* **1973**, *38*, 3916−3918. (b) Ford, W. T.; Hart, D. J. *J. Phys. Chem.* **1976**, *80*, 1002−1004.

(38) (a) Cooper, E. I.; Angell, C. A. *Solid State Ionics* **1983**, *9 & 10*, 617−622. (b) Cooper, E. I.; Angell, C. A. *Solid State Ionics* **1983**, *18 & 19*, 570−576.

(39) Henderson, W. A.; Passerini, S. *Chem. Mater.* **2004**, *16*, 2881−2885.

(40) (a) Vogel, H. *Phys. Z.* **1921**, *22*, 645. (b) Fulcher, G. S. *J. Am. Ceram. Soc.* **1923**, *8*, 339−355. (c) Tamman, G.; Hesse, W. *Z. Anorg. Allg. Chem.* **1926**, *156*, 245−257.

(41) (a) Ue, M. *J. Electrochem. Soc.* **1994**, *141*, 3336−3342. (b) Ue, M.; Murakami, A.; Nakamura, S. *J. Electrochem. Soc.* **2002**, *149*, A1385−A1388.

(42) The van der Waals cationic size of [bmim], [bmpro], and [(*n*-C_4H_9)-(CH_3)$_3$N] was not available in the literature. However, cationic size of [emim], [empro], and [(C_2H_5)(CH_3)$_3$N] has been reported as 116, 133, and 110 Å^3 (0.303, 0.317, and 0.297 nm), respectively.[41b] Therefore, the cationic size of [bmim], [bmpro], and [(*n*-C_4H_9)(CH_3)$_3$N] may be approximated by considering that an increase in one methylene unit (−CH_2−) in the alkyl substituent of the tetraalkylammonium cation brings about an increase in the cationic volume (radius) of about 17 Å^3 (0.160 nm).

(43) Baker, S. N.; Baker, G. A.; Bright, F. V. *Green Chem.* **2002**, *4*, 165−169.

(44) Kaar, J. L.; Jesionowski, A. M.; Berberich, J. A.; Moulton, R.; Russesll, A. J. *J. Am. Chem. Soc.* **2003**, *125*, 4125−4131.

(45) (a) Reichardt, C. *Chem. Rev.* **1994**, *94*, 2319−2358. (b) *Solvents and Solvent Effects in Organic Chemistry*, 3rd ed.; Reichardt, C., Ed; Wiley-VCH: Weinheim, 2003.

(46) (a) Kamlet, M. J.; Taft, R. W. *J. Am. Chem. Soc.* **1976**, *98*, 377−383. (b) Taft, R. W.; Kamlet, M. J. *J. Am. Chem. Soc.* **1976**, *98*, 2886−2894. (c) Kamlet, M. J.; Abboud, J. L.; Taft, R. W. *J. Am. Chem. Soc.* **1977**, *99*, 6027−6038. (d) Kamlet, M. J.; Abboud, J. L.; Abraham, M. H.; Taft, R. W. *J. Org. Chem.* **1983**, *48*, 2877−2887.

(47) Tsuzuki, S.; Tokuda, H.; Hayamizu, K.; Watanabe, M. *J. Phys. Chem. B* **2005**, *109*, 16474−16481.